Synthesis and Structure−Property Investigation of Polyarenes with Conjugated Side Chains

Hairong Li, Manoj Parameswaran, Muhammad Hanafiah Nurmawati, Qinghua Xu, and Suresh Valiyaveettil*

Department of Chemistry, National University of Singapore, 3 Science Drive 3, Singapore 117543, Singapore

Received July 7, 2008; Revised Manuscript Received September 16, 2008

ABSTRACT: A series of cross-conjugated polyarenes were synthesized and fully characterized. The polymers were soluble in common organic solvents and showed good thermal stability. Powder XRD showed ordered structures for all polymers and significant shift in the emission maxima with increasing concentration, indicating strong aggregation of polymer chains in solution. Solvatochromism studies showed blue shifts of absorption and fluorescence maxima in toluene as compared to the values in THF, suggesting that polymers tend to aggregation less or solvated more in toluene. A large two-photon absorption (TPA) cross section was observed for all polymers due to the unique molecular architectures. Fluorescence lifetime studies revealed that aggregation induced fast decay kinetics. Self-assembled helical nanofibers and nanorings were observed when casted films from polymer solutions. HRTEM and XRD investigation of the thin films revealed nanocrystalline structures of the polymers.

Introduction

A large variety of conjugated organic compounds have been synthesized, and properties were studied for potential applications in areas such as light-emitting diodes (LEDs),[1,2] field effect transistors (FET),[3] photovoltaic cells,[4,5] and optical sensors.[6] Besides the commonly studied linear conjugated polymers and oligomers, molecules based on cross-conjugated platforms have been gaining great interest in the past few years.[7−11] Such polymers are usually divided into two classes based on the structure: acyclic systems such as dendralenes,[12−16] iso-polydiacetylenes,[17,18] iso-polytriacetylenes,[19−21] poly(phenylenevinylidene)s,[22−24] and cyclic systems mainly referred to radialene derivatives.[25−34] Recently, a novel series of water-soluble cross-conjugated poly(*p*-phenylenes) (PPPs) was reported by our group, with interesting aggregation behavior in water driven by electrostatic and $\pi-\pi$ interactions.[6] Specifically, our interest lies in understanding how and to what extent the $\pi-\pi$ interaction affects the photophysical properties of cross-conjugated polymers. Here, a series of soluble polymers with cross-conjugation along the polymer backbone (Figure 1) were designed and synthesized. This strategy provides a route for tuning the optical properties of the polymers by extending the conjugation length in two dimensions.[35−47] It is anticipated that the structure of the polymer backbone should possess strong $\pi-\pi$ interactions among the polymer chains, which enhances self-assembly induced planarization in solid state. Furthermore, useful information could be elicited through investigation of relationship between rigid backbone and flexible bisdiene side chain. Our strategy offers a new approach for introducing different conjugated side chains onto the polymer backbone for enhancing cross-conjugation, fine-tuning optical properties with an added flexibility to incorporate multiple functional groups such as electron-donating/withdrawing groups on the conjugated side chains.

Experimental Section

Instruments. The NMR spectra were collected on a Bruker ACF 300 spectrometer in chloroform-*d*, tetrahydrofuran-d_8 (THF-d_8) as solvent, and tetramethylsilane as internal standard. FT-IR spectra were recorded on a Bio-Rad FTS 165 spectrophotometer using KBr matrix. UV−vis spectra were recorded on a Shimadzu 3101 PC spectrophotometer, and fluorescence measurements were carried out on a RF-5301PC Shimadzu spectrofluorophotometer. Thermogravimetric analyses were done using TA Instruments SDT 2960 with a heating rate of 10 °C/min up to 1000 °C under a nitrogen atmosphere. Gel permeation chromatography (GPC) was used to obtain the molecular weight of the polymers with reference to polystyrene standards using tetrahydrofuran (THF) as solvent. Elemental analyses were performed using a Perkin-Elmer CHNS autoanalyzer. X-ray powder patterns were obtained using a D5005 Siemens X-ray diffractometer with Cu Kα (1.54 Å) radiation (40 kV, 40 mA). Samples were mounted on a sample holder and scanned between $2\theta = 1.5°$ and 40° with a step size of $2\theta = 0.02°$. Dynamic light scattering (DLS) studies were carried out with 90 Plus particle size analyzer (Brookhaven Instruments). The data were collected at a scattering angle of 90° to the incident laser beam with power of 35 mW and wavelength of 678 nm. The NNLS method was used to analyze the first-order field correlation function for size distribution. SEM images were taken with a JEOL JSM 6700 scanning electron microscope. HRTEM images were taken using a JEOL 3010 at an accelerating voltage of 300 kV. The samples were carefully mounted on copper stubs with a double-sided conducting carbon tape and sputter-coated with platinum (2 nm) before examination. Fluorescence lifetimes were measured using time-correlated single-photon counting technique (TCSPC). The frequency-doubled output of a mode-locked Ti:sapphire laser (Tsunami, Spectra-Physics) was used for excitation of the sample at 400 nm. The output pulses from Ti:sapphire centered at 800 nm had a duration of 40 fs with a repetition rate of 80 MHz. The Ti:sapphire laser was pumped by 5 W output of a frequency-doubled diode Nd:YVO_4 laser (Millennia Pro, Spectra-Physics). For fluorescence lifetime measurements, the fluorescence intensity was collected by an optical fiber which is directed to an avalanche photodiode (APD). The signals were processed by a PicoHarp 300 module (PicoQuant). The system gives a temporal resolution of ∼100 ps.

Materials. All reagents were purchased from Sigma-Aldrich, Fluka, Lancaster, or TCI and were used without further purification unless otherwise stated. All reactions were carried out with dry, freshly distilled solvents under anhydrous conditions or in an inert atmosphere. Silica gel was used as packing material for column purification. Tetrahydrofuran (THF) was purified by distillation over sodium under a nitrogen atmosphere.

* To whom correspondence should be addressed: Tel (65) 65164327, Fax (65) 67791691, e-mail chmsv@nus.edu.sg.

10.1021/ma801506c CCC: $40.75
Published on Web 10/24/2008

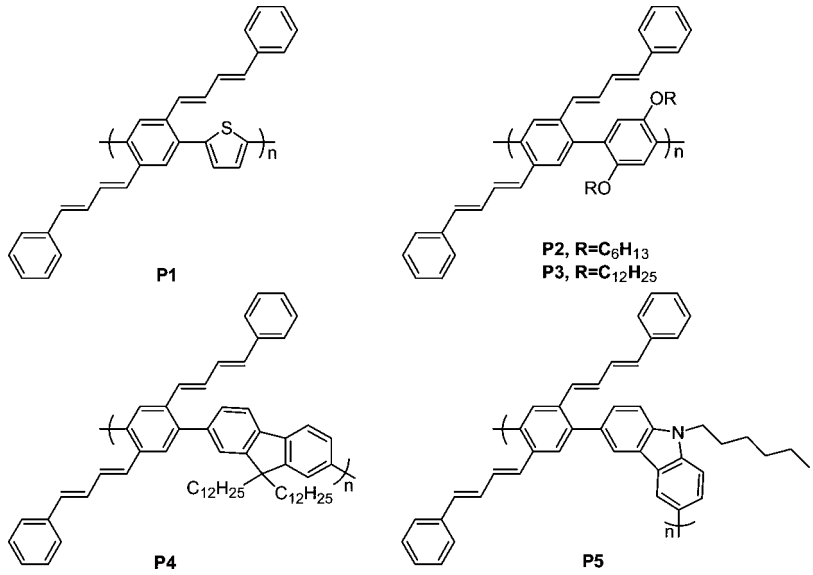

Figure 1. Structures of target polymers.

Synthesis. The synthetic routes to the polymers are given in Scheme 1. 2,5-Dibromo-*p*-xylene, hydroquinone, 2,7-dibromofluorene, and carbazole were used as starting materials. 1,4-Dibromo-2,5-bis-bromomethyl-benzene (**2**),[48] 2,5-dibromohydroquinone (**6**),[49] 2,5-dibromo-1,4-dialkoxybenzene (**7**),[50] 2,7-dibromo-9,9-bisdodecyl-9*H*-fluorene (**10**),[51] 3,6-dibromocarbazole (**13**),[52] 3,6-dibromo-9-hexyl-9*H*-carbazole (**14**),[53] and all the corresponding diboronic acids (**8**, **11**, **15**)[54,55] were synthesized according to the reported procedures.

*1,4-Dibromo-2,5-bis(4-phenylbuta-1,3-dienyl)benzene (**4**).* A mixture of compounds **2** (2 g, 4.8 mmol) and triethylphosphite (3.3 mL, 19.2 mmol) was refluxed for 6 h, and the excess triethylphosphite was removed under reduced pressure. The obtained 2,5-dibromo-4-(diethoxyphosphorylmethyl)-benzyl]phosphonic acid diethyl ester (**3**) was dissolved in dry DMF (25 mL) and mixed with potassium *tert*-butoxide (1.8 g, 19.2 mmol) and cinnamaldehyde (3.6 mL, 28.8 mmol). The mixture was stirred overnight at 50 °C, poured into water, and filtered, and the crude solid was recrystallized from methanol, giving a yellow product with 75% yield.

^{1}HNMR (THF-d_8, δ ppm): 7.57−7.70 (m, 6H central Ar−H, terminal Ar−H), 7.30 (t, J = 7.5 Hz, 4H terminal Ar−H), 7.18 (t, J = 7.2 Hz, 2H, on terminal Ar−H), 6.90−6.96 (m, 4H, diene-H), 6.85 (d, J = 15.1 Hz, 2H, diene-H), 6.78 (d, J = 15.3 Hz, 2H, diene-H). ^{13}C NMR (THF-d_8, δ ppm): 138.1, 136.0, 134.1, 130.8, (Ar−C), 129.8, 129.3, 128.6, 128.0, 127.4, 126.9, 126.5, (Ar−C and diene-C). FTIR (KBr, cm^{-1}): 3022, 2924, 1753, 1610, 1458, 1446, 1365, 1053, 983, 887, 856, 821, 746, 684, 503. Elemental analysis: C: 63.44, H: 4.10, Br 32.47. Found: C: 63.04, H: 4.41, Br 32.16.

*Poly(2,5-bis(4-phenylbuta-1,3-dienyl)-1,4-phenylene-alt-1,4-thiophene) (**P1**).* Thiophene-2,5-diboronic acid (0.41 g, 2.34 mmol) and compound **4** (1 g, 2.34 mmol) were dissolved in 30 mL of THF. K_2CO_3 solution (2 M, 20 mL) was added to the mixture followed by tetrakis(triphenylphosphino)palladium(0) (3 mol %) as catalyst and cetyltrimethylammonium bromide (30 mol %) as phase transfer agent. The mixture was stirred at 70 °C for 3 days, concentrated, and precipitated twice from methanol, and the crude product was further purified by filtration through silica gel using dichloromethane (DCM).

P1: ^{1}H NMR ($CDCl_3$, δ ppm): 7.73 (b, 2H, central Ar−H), 7.38−7.45 (b, 6H, terminal Ar−H, Thio−H), 7.31 (b, 4H, terminal Ar−H), 7.10−7.18 (b, 4H, terminal Ar−H, Th−H), 6.89−6.96 (b, 6H, diene−H), 6.73 (b, 2H, diene−H).^{13}C NMR ($CDCl_3$, δ ppm): 142.0 (Th−C), 137.2, 134.0, 133.2., 133.0, 131.6, 130.9, 130.4 (Th−C and Ar−C), 129.3, 128.6, 128.1, 127.7, 126.3, 125.9 (Ar−C, Th−C, and diene−C). FTIR (KBr, cm^{-1}): 3021, 2954, 2920, 2855, 1724, 1629, 1599, 1479, 1434, 1384, 1360, 1241, 1091, 1022, 983, 872, 805, 746, 690, 622, 509. Elemental analysis: C: 86.5, H: 6.09, S: 7.45. Found: C: 85.9, H: 6.63, S: 7.90.

P2: ^{1}H NMR ($CDCl_3$, δ ppm): 7.62−7.70 (b, 6H, central Ar−H, terminal Ar−H), 7.55 (b, 2H, OAr−H), 7.30 (b, 4H, terminal Ar−H), 7.19 (b, 2H, terminal Ar−H), 6.90−6.99 (b, 6H, diene−H), 6.65 (b, 2H, diene−H)), 3.90 (b, ArOC**H**$_2$CH$_2$), 1.82 (b, ArOCH$_2$C**H**$_2$), 1.26 (b, (C**H**$_2$)$_3$CH$_3$), 0.90 (b, C**H**$_3$).^{13}C NMR ($CDCl_3$, δ ppm): 150.9, 140.5, (OAr−C), 138.4, 136.2, 134.7, 132.0, 130.2, 130.1, (Ar−C and OAr−C), 129.2, 128.7, 127.9, 126.5, 125.4, 116.4, (Ar−C, OAr−C, and diene−C), 69.5, 31.4, 29.3, 25.5, 22.5, 14.7 (Alk−C). FTIR (KBr, cm^{-1}): 3025, 2953, 2926, 2856, 1729, 1593, 1498, 1467, 1378, 1261, 989, 866, 800, 748, 690, 621, 507. Elemental analysis: C: 85.5, H: 8.23; Found: C: 84.85, H: 8.74.

P3: ^{1}H NMR ($CDCl_3$, δ ppm): 7.58−7.73 (b, 8H, central Ar−H, terminal Ar−H, OAr−H), 7.29 (b, 4H, terminal Ar−H), 7.18 (b, 2H, terminal Ar−H), 6.93 (b, 6H, diene−H), 6.69 (b, 2H, diene−H), 3.90 (b ArOC**H**$_2$CH$_2$), 1.80 (b, ArOCH$_2$C**H**$_2$), 1.24 (b, (C**H**$_2$)$_3$CH$_3$), 0.88(b, C**H**$_3$).^{13}C NMR ($CDCl_3$, δ ppm): 151.9, 140.7, (OAr−C), 138.0, 136.1, 133.6, 132.4, 130.5, 130.1, (Ar−C and OAr−C), 129.3, 128.5, 127.5, 126.2, 125.4, 118.2, (Ar−C, OAr−C, and diene−C), 68.4, 31.8, 29.6, 27.2, 25.7, 22.5, 14.7 (Alk−C). FTIR (KBr, cm^{-1}): 3025, 2922, 2852, 1729, 1592, 1484, 1468, 1378, 1261, 1214, 1028, 990, 868, 803, 784, 721, 690, 618, 506. Elemental analysis: C: 86.3, H: 9.54. Found: C: 85.71, H: 9.89.

P4: ^{1}H NMR ($CDCl_3$, δ ppm): 7.70−7.84 (b, 6H, central Ar−H, Fl−H), 7.38−7.50 (b, 12H, Fl−H), 7.20−7.29 (b, terminal Ar−H, C**H**Cl$_3$), 6.90−7.02 (b, 6H, diene−H), 6.74 (b,2H, diene-H), 3.60 (b, C**H**$_2$ connected to sp^3 carbon on fluorene), 2.00 (b, C**H**$_2$ next to CH$_2$ connected to sp^3 carbon on Fl−H), 1.25 (b, (C**H**$_2$)$_9$CH$_3$), 0.87 (b, C**H**$_3$).^{13}C NMR ($CDCl_3$, δ ppm): 150.5, 141.5, (Fl-C), 140.7, 139.2, 137.2, 134.4, 131.0, 130.2, (Fl−C and Ar−C), 129.3, 128.5, 128.2, 127.4, 126.2, 125.4, 124.7, 123.6, 119.7, (Fl−C, diene−C, and Ar−C), 40.2, 31.5, 29.7, 23.8, 22.5, 14.7 (Alk−C). FTIR (KBr, cm^{-1}): 3022, 2922, 2850, 1726, 1592, 1458, 1373, 1260, 1118, 1025, 983, 893, 823, 747, 688, 621, 536, 505. Elemental analysis: C: 90.50, H: 9.49. Found: C: 90.05, H: 9.72.

P5: ^{1}H NMR ($CDCl_3$, δ ppm): 8.21 (b, 2H, Cz−H), 7.82 (b, 2H, central Ar−H), 7.47−7.60 (m, 4H, Cz−H), 7.24−7.33 (b, terminal Ar−H, C**H**Cl$_3$), 7.16 (b, 2H, terminal Ar−H), 6.85−6.99 (b, 6H, diene−H), 6.62 (b, 2H, diene−H), 4.37 (b, NC**H**$_2$), 1.95 (b, NCH$_2$C**H**$_2$), 1.36 (b, (C**H**$_2$)$_3$CH$_3$), 0.91 (b, CH$_2$C**H**$_3$). ^{13}C NMR ($CDCl_3$, δ ppm): 140.8, 139.6, 134.5, 132.2, 131.6, 130.4, (Cbz−C and Ar−C), 129.8, 129.2, 128.4, 127.2, 126.2, 122.7, 121.4, 120.5,

Scheme 1. Synthetic Routes to P1−P5

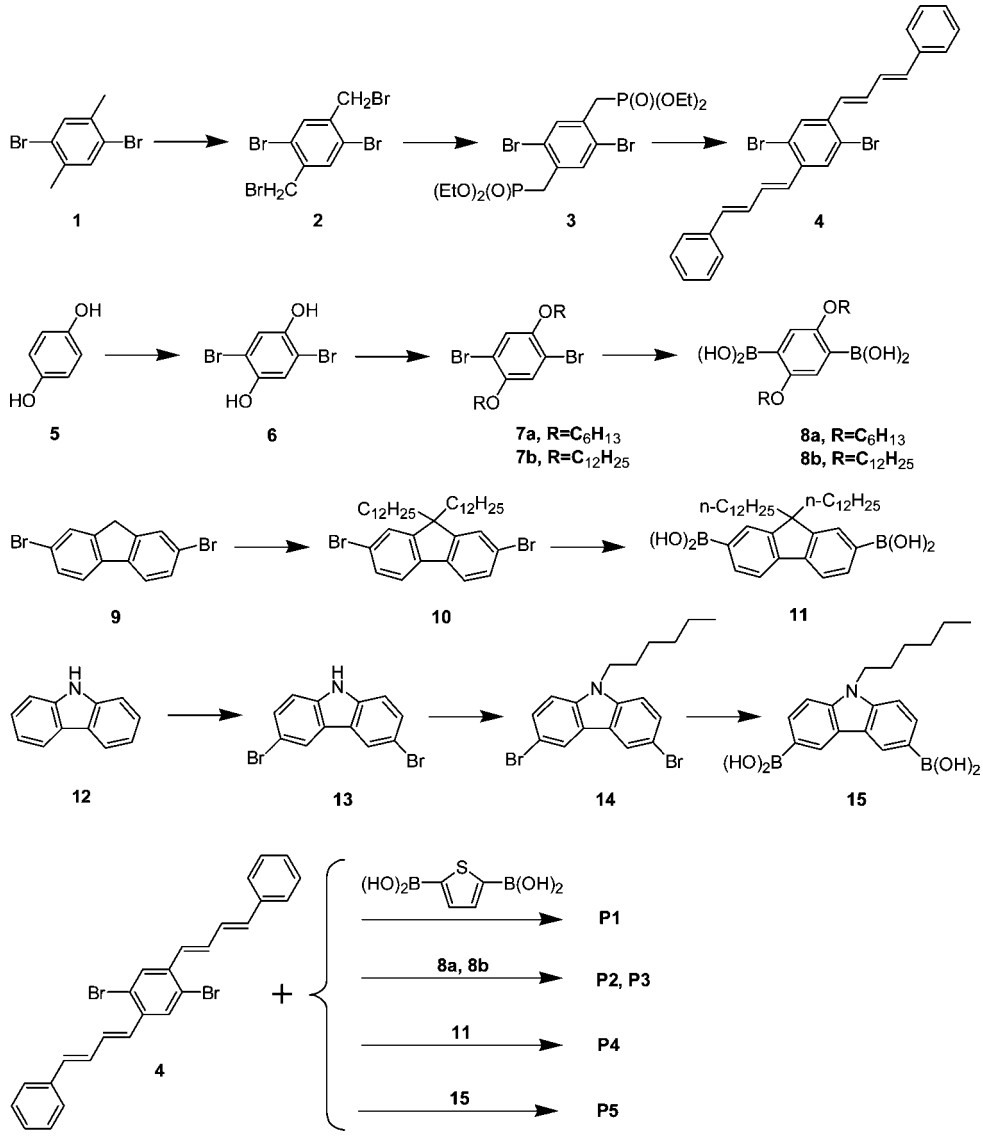

Table 1. Molecular Weights and T_d Values of P1−P5

polymer	M_n	M_w	M_w/M_n (PDI)	T_d (°C)
P1	5900	7 500	1.27	250
P2	6200	9 600	1.55	325
P3	8800	11 700	1.33	337
P4	6700	10 800	1.61	285
P5	5700	10 200	1.79	370

118.9, 108.7, (Cbz−C, Ar−C, and diene−C), 44.2, 32.5, 29.0, 27.0, 23.2, 14.7 (Alk−C). FTIR (KBr, cm^{-1}): 3023, 2923, 2852, 1858, 1726, 1683, 1597, 1474, 1378, 1348, 1260, 1216, 1150, 1065, 887, 805, 747, 691, 624, 505. Elemental analysis: C: 90.4, H: 7.25, N: 2.34. Found: 89.89, H: 7.75: N: 2.47.

Characterization. All polymers showed good solubility in common organic solvents such as THF, dichloromethane (DCM), dimethylformamide (DMF), and toluene. But monomer **4** (Scheme 1) was less soluble in the above-mentioned solvents. By incorporating a second soluble monomer (i.e., boronic acids), soluble target polymers were obtained. Molecular weights of all polymers were determined using gel permeation chromatography with reference to polystyrene standards using THF as solvent. The obtained values were in the range of $(5.7-8.8) \times 10^3$ (M_n) with polydispersity index (PDI) of 1.27−1.79 (Table 1).

Thermogravimetric analysis (TGA) was done using a heating rate of 10 °C/min up to 1000 °C under a N_2 atmosphere. All polymers showed reasonably good thermal stability (Table 1) up to 250 °C. The decomposition temperatures varied among polymers and **P1** showed lowest stability due to the presence of thiophene units. All polymers decomposed through a one-step process except the **P4** which showed a two-stage decomposition; this may be due to the initial decomposition of long dodecyl alkyl chains on fluorene.[50]

Powder X-ray Diffraction. Polymers **P2** and **P3** possess organized packing structures shown in Figure 2. The strong peaks in the low-angle region seem to correspond to a distance between the polymer backbone separated by the side chain, indicating a long-range order.[50,54] There is a sharp peak at $2\theta = 4.45°$ ($d = 19.2$ Å) for **P2**, while **P3** has two peaks: $2\theta = 2.59°$ ($d = 26.0$ Å) and $3.33°$ ($d = 33.9$ Å); it appears that there are two packing structures. The presence of alternative side chains with different length on the polymer backbone of **P3** led to two sharp peaks in the low-angle region: one involves partial interdigitation and the other one comprises end-to-end packing of side chains (Figure 2b,c).[54] The broad peaks at the high-angle region (20°−30°) for all polymers were originated from the face-to-face distance between loosely packed side chains.[55,56] Note that the difference in peak positions (33.9 and 26.0 Å) in the XRD pattern of **P3** is about 7.9 Å, which can be assigned to the length of six C−C bonds in *all-trans* conformation. This is consistent to our proposed packing model.

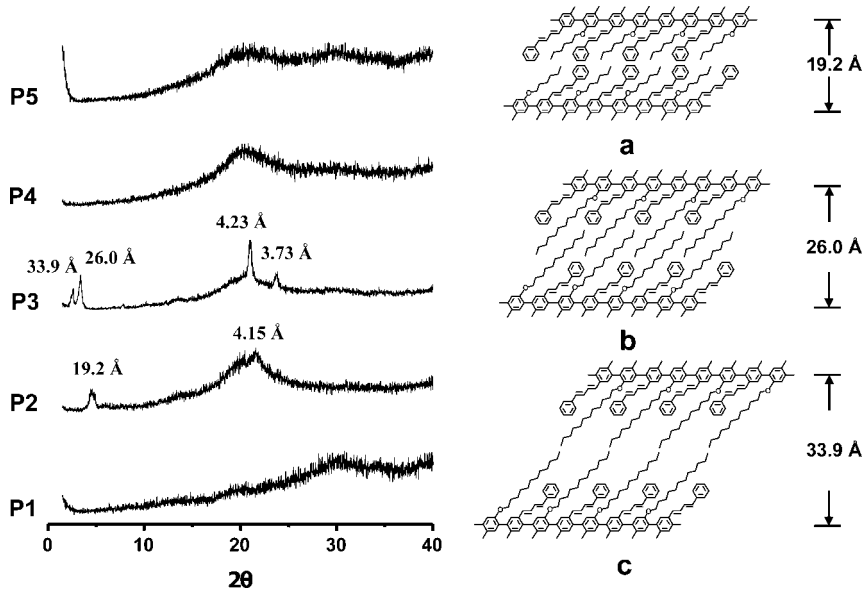

Figure 2. Left: powder XRD spectra for **P1** to **P5**; right: schematic diagrams of possible packing structures for **P2** (a, double degeneracy) and **P3** (b, c).

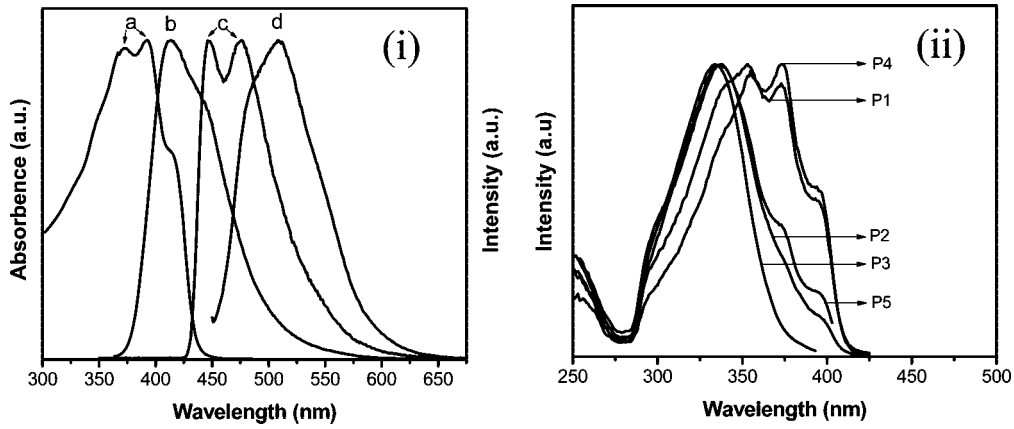

Figure 3. (i) Normalized absorption (a) and emission (b) spectra of **P3** at a low concentration in THF (0.002 g/L), emission spectra of **P3** at high concentration in THF (*c*, 0.2 g/L) and for spin-coated thin film (d). (ii) Excitation spectra of **P1**−**P5** monitored at the emission peaks at a low concentration.

Table 2. Absorption Maxima of the Polymers in THF, Emission Maxima at Low (P_L) and High (P_H) Concentrations in THF, Thin Film (P_N), and Excitation Maxima (P_E)

polymer	P1	P2	P3	P4	P5
1st local ABS_{max} (nm)	394	394	398	387	396
2nd local ABS_{max} (nm)	374	374	372	370, 340	374
P_L (nm)	433	422	414	418	438
P_H (nm)	486	451	447, 475	456	469
P_N (nm)	542	511	509	503	508
P_E (nm)	353, 373	337	334	355, 373	337

Results and Discussion

Absorption and Emission. Absorption and emission spectra of all polymers were done in THF solution at a concentration of 0.002 g/L (Figure 3, Figure S2 in Supporting Information, and Table 2). All UV−vis spectra showed broad absorption maxima at 374 and 394 nm, which could be assigned to the $\pi \rightarrow \pi^*$ transition of phenylene backbone and diene side chains, respectively. Compared to conventional PPPs which shows an absorption maximum approximately at ca. 340 nm,[50,57–59] the absorption maxima of **P1**−**P5** showed significant red shift, indicating extended conjugation (Table 2). This implies a more planar structure due to the cross-conjugation and the effective packing of polymer chains, which is different from packing of adjacent phenylene rings on the backbone.[60] The absorption maxima were similar for **P1**, **P2**, **P3**, and **P5** (Table 2), while **P4** showed a blue shift in absorption maximum with a third absorption peak at 348 nm. This is due to the steric hindrance of adjacent side chains, which leads to a nonplanar conformation for the polymer backbone of **P4**, as observed for other polymers.[61,62] When comparing the excitation spectra with UV−vis absorption spectra, it is obvious that the maximum absorption peaks for the polymers did not correspond to optimal excitation wavelength. **P2**, **P3**, and **P5** showed excitation peak around 340 nm, about 50 nm blue-shifted compared to the corresponding UV−vis absorption maxima (Table 2, P_E). It was anticipated that the backbone (PPP) was highly twisted relative to planar conjugated side chain, which reflected the presence of two orthogonal chromophores weakly interacting with each other. Excitation could be initiated in the side chain chromophore with higher band gap, which was then transferred to the one with lower band gap. Because of less effective conjugation between side chain and backbone, it might result in disjoint nature of HOMOs and LUMOs of side chain from backbone; the shorter transition could be largely forbidden, while the emission from this state is due to the vibrational relaxation.[63]

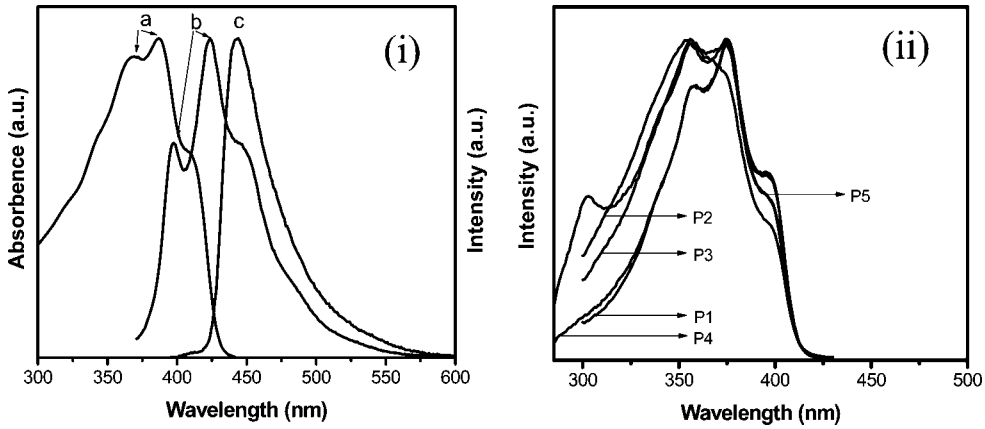

Figure 4. (i) Normalized absorption (a) and emission (b) spectra of **P3** at a low concentration in toluene (0.002 g/L), emission spectra of **P3** at high concentration in toluene (*c*, 0.2 g/L). (ii) Excitation spectra of **P1**−**P5** recorded at the emission peaks at a low concentration.

Table 3. Absorption (ABS_{max}) and Emission Maxima of the Polymers at Low (P_L) and High (P_H) Concentrations in Toluene and Excitation Maxima (P_E)

polymer	P1	P2	P3	P4	P5
1st local ABS_{max} (nm)	384	387	386	387	391
2nd local ABS_{max} (nm)	374	368	367	374, 342	373
P_L (nm)	427	432	423	430	444
P_H (nm)	476	445	443	455	457
P_E (nm)	377	357	356, 375	357, 376	356, 375

Emission characteristics of the polymers were measured at a low (0.002 g/L) and a high (0.2 g/L) concentration in THF (Figure 3ii, Figure S2 in Supporting Information, and Table 2). At a low concentration, all polymers showed the emission peaks between 414 and 438 nm, with significant overlaps with their respective absorption peaks. However, the excitation spectra for all polymers showed that the optimal excitation wavelength, which gives highest emission intensity, was averaged around 350 nm rather than 390 nm, where the absorption intensity was maximum. This is not surprising for polymers with a strong charge transfer character.[59,64]

It is well-known that in polymer solids[65–67] and polymer blends[68,69] the intermolecular interactions via photon-induced charge separation, formation of excimer, exciplexes, or aggregates become more efficient. This leads to a red shift or generation of a new peak on the longer wavelength region and reduces the quantum efficiency of fluorescence. At a high concentration of 0.2 g/L, **P1** showed a single peak at 486 nm (Table 2) with a red shift of more than 50 nm as compared with that in low concentration (0.002 g/L). This should be attributed to the formation of the intermolecular complex of the polymer.[70,71] Other concentrations in between were also studied with observed peak maxima in between as well with large overlap, but not in a linear relation. The ideal discrete aggregation state could not be confirmed. A significant red shift of more than 100 nm in emission maximum (542 nm) was observed in the solid state due to enhanced intermolecular order in the aggregates,[64] as compared with that in dilute solution (433 nm). **P3** showed two emission peaks at high concentration (447 and 475 nm, Figure 3), which might be due to the nonplanar structures as well as the coexistence of two intermolecular complexes resembling its powder XRD pattern (**P3** in Figure 2).

In order to examine the solvent influence on aggregation, UV−vis, fluorescence, and excitation spectra of the polymers were recorded in nonpolar toluene (Figure 4, Figure S3 in Supporting Information, and Table 3) and compared with the data obtained in polar THF solution. In UV−vis spectra, absorption peaks of all polymers showed a blue shift of 5−10 nm in toluene, indicating a relatively lower degree of intermolecular interaction. For fluorescence spectra, all polymers showed well-defined peaks at low concentrations in toluene as compared to those in THF solution with no significant changes in emission maxima. At high concentration in toluene, where the aggregation was expected, all polymers showed a red shift of the emission maxima, but to less extent than those in THF due to the change in polarity.[72] For example, **P1**, **P2**, and **P5** showed red shifts in the range of 6−12 nm. **P3** and **P4** did not show any significant change in the emission maximum (Tables 2 and 3) probably due to the presence of longer alkyl chains. However, dynamic light scattering (DLS) studies showed a clear bimodal distribution of aggregate size at 5 and 50 nm at a high concentration for all polymers in both THF and toluene (Figure 5 and Figure S4 in Supporting Information). Morphological studies using scanning electron microscope (SEM), as discussed later in the paper, showed fibrous and ring type morphologies at different concentrations. These observations indicated interplay of two competitive forces between polymer chains and solvent molecules expected to control the intermolecular interactions.

In toluene, the polymer chains are less ordered because of strong salvation of individual polymer chains by solvent molecules especially for **P1** with no alkyl chains, which results in less charge transfer among the polymer aggregates, regardless of the size of the aggregates. While THF solvates the polymer chains with alkyl chains, it has no significant effect on the $\pi-\pi$ interaction between polymer chains, resulting in a more ordered assembly. The most obvious change was the excitation spectra, where the peak maxima of **P2**, **P3**, and **P5** showed significant red shifts (between 356 and 375 nm, Table 3) in toluene as compared with the values in THF. This indicated that nonpolar toluene molecules had a low dipole colliding relaxation effect on excited states and disjoint nature of frontier molecular orbits (FMOs) of less conjugated chromophores.

An experiment was carried out where polarity of the solvent gradually decreased (Figure 6). It was found that with addition of bad solvent hexane into to the THF solution of **P3** the absorption maxima gradually shifted to higher wavelength, and so did the emission maxima. The intensity of emission also gradually decreased due to aggregation. At the ratio of hexane: THF = 8:2, a collapse of absorption spectra was observed, which was probably due to partial precipitation. These results indicated that the red shifts in both absorption and emission spectra might be dominated by aggregation rather than the structural planarization. However, it should be again emphasized that strong aggregation and structural planarization of polymer backbone are interrelated to each other.[73,74]

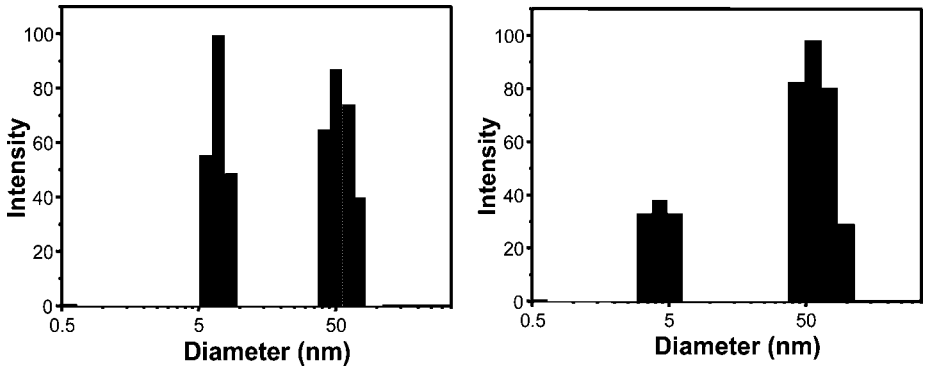

Figure 5. DLS results of **P3** in THF (left) and toluene (right) at concentration of 0.2 g/L.

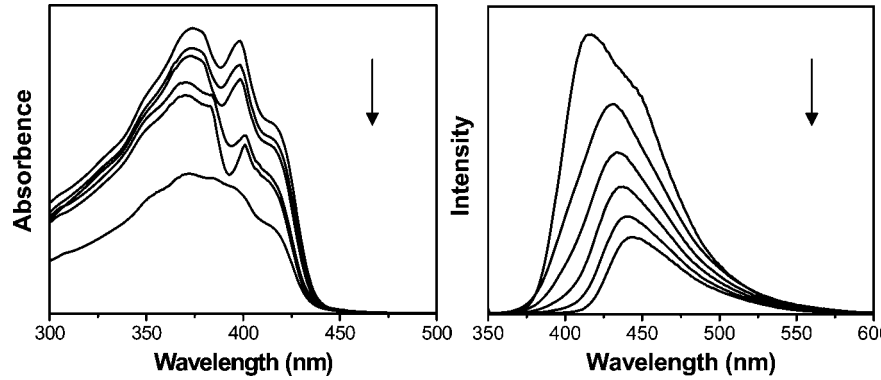

Figure 6. Absorption (left) and emission (right) spectra of **P3** in THF and hexane solvent mixture. Volume % of hexane: 0%, 20%, 35%, 50%, 65%, and 80%. Polymer concentration was 5 mg/L.

Table 4. Quantum Yield (QY) and Absolute and Relative Values of TPA Cross Section for P1−P5 in THF and Toluene[a]

solvent	polymer	GM at 800 nm	δ/δ_{Rh}	QY (%)	solvent	solymer	GM at 800 nm	δ/δ_{Rh}	QY (%)
toluene (2.4)	**P1**	1640	10.9	2.5	THF(4.0)	**P1**	1215	8.1	2.0
	P2	877	5.8	6.3		**P2**	1121	7.5	4.7
	P3	1159	7.7	8.6		**P3**	1698	11.3	5.6
	P4	2196	14.6	3.3		**P4**	3210	21.4	2.3
	P5	753	5.0	8.1		**P5**	630	4.2	7.2

[a] Polarity is indicated in parentheses; rhodamine B was used as standard.

Fluorescence Quantum Yield and Two-Photon Absorption (TPA). Quantum yield measurements were carried out in toluene and THF; quinine sulfate was used as standard (Table 4). The existence of disjoint nature of FMOs promoted the vibrational relaxation to lower state before emission; in other words, energy was lost during inner transfer as explained by excitation spectra. Second, the polymers were generally low in solubility even in good solvent, which probably induce the cluster formation to minimize the exposure of unfavorable aromatic part, as is always the case of water-soluble conjugated PPPs;[6] thus, the intermolecular interaction further dissipated the energy.[75] Furthermore, although the polymer backbones are rigid in nature, *trans*-diene side chains could undergo dramatic conformational changes upon excitation, migration of excited-state to "soft" chromophore followed by relaxation should account for the low quantum efficiency.[76] The TPA cross section was measured by two-photon-induced fluorescence (TPIF) and calculated using the equation given in the literature.[77] In spite of low quantum yield, they exhibited high TPA cross sections (Table 4) compared with the standard rhodamine B in ethanol (quantum yield = 70%, $\delta = 150 \pm 50 \times 10^{-50}$ cm^4 s/photon[78,79]). The two-photon absorption property of materials depends on at least three factors. First of all, the polymers obey the "push−push" quadrupolar charge transfer structure where the two electron donors (thiophene, alkoxylphenylene, carbazole, etc.) were linked to the rigid center, which showed intense TPA.[80,81] All these donors were stringed by the rigid PPP backbone which provided additive effect on TPA. The extended conjugation through bisdiene side chain offers large polarization which led to increase in TPA.[82–84] The system could be described as the coexistence of "push−push" along backbone and "push−pull" from backbone to side chain, which indicates that further improvement could be done by introducing strong electron-withdrawing group on the conjugated side chain.[85–87] Materials with large two-photon absorption cross sections are of interest in the application of optical limiting,[88] 3D optical data storage,[89] microfabrication,[90] and photodynamic therapy,[91] etc.

Fluorescence Lifetime Measurements. The excited-state lifetimes of these polymers (**P1**−**P5**) were measured using the time-correlated single photon counting technique (TCSPC). The decay profile was measured in two solvents: toluene and THF. The detection wavelength was chosen at 450 nm where the emission of monomeric and aggregated systems to overlap. Table 5 summarizes the fitting data (decay time and amplitude) of the fluorescence decay curves for all polymers in toluene and THF. It was observed that at a low polymer concentration (10^{-7} M) **P3** showed a monoexponential decay in both solvents indicating monomeric emission. For **P1**, **P4**, and **P5**, the excited-state decay comprises more than a single-exponential component. At least two exponential components are needed to fit the data, indicating formation of aggregate/excimer, which leads in shortening of the excited-state decay, usually a faster initial

Table 5. Decay Time (τ) and Amplitude (a) for Fluorescence Decay at Concentration of 10^{-7} M

	toluene				THF			
polymer	$a(1)$	$\tau(1)^a$	$a(2)$	$\tau(2)$	$a(1)$	τ (1)	$a(2)$	$\tau(2)$
P1	0.41	461.24	0.59	1033.64	0.17	714.6	0.83	1221.99
P2	1	1325.28			1	930.30		
P3	1	1211.69			0.56	146.22	0.44	1226.31
P4	0.85	117.77	0.15	996.27	0.6	138.71	0.4	1163.48
P5	0.28	794.99	0.72	1397.03	0.12	952.43	0.88	1283.11

[a] All in picoseconds; a = amplitude; τ = lifetime.

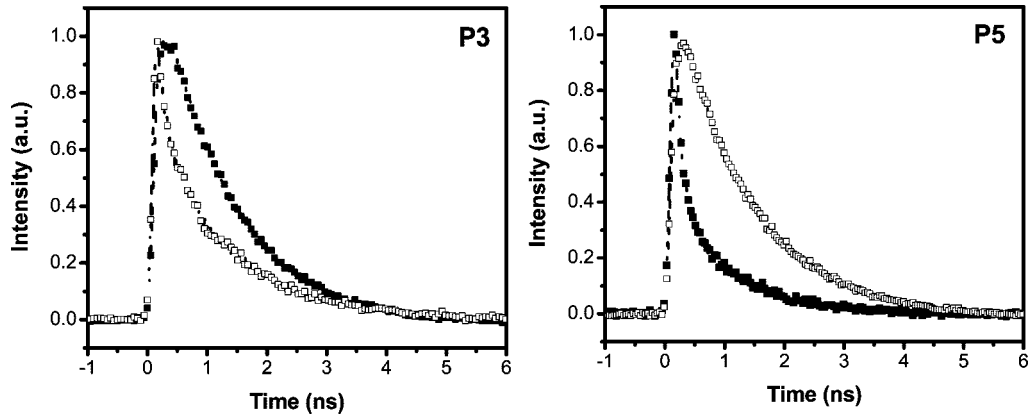

Figure 7. Fluorescence decay curves of **P3** and **P5** in toluene (■) and THF (□) monitored at 450 nm at concentration of 10^{-7} M.

decay followed by a slower process, as compared to the monomer. The fast decay is usually ascribed to energy transfer from single excited fluorophores to aggregates.[90] Polarity of solvent had strong effect on the decay profile as shown in Figures 7 and S5, depending on the solvent and polymer. **P3** in THF has faster decay probably due to long alkyl chain. It was found that the solubility of **P3** was much better than others in toluene, which should be due to the long alkyl chain. Meanwhile, the $\pi-\pi$ interaction between polymer chain and numerous toluene molecules around should also participate in the energy dissipation. The opposite trend was observed for **P5** with poorer solubility in toluene and electron active carbazole group attributed to strong dipole interaction with polar solvent.

Solid Phase Self-Assembly and Morphology Studies. The polymer has very good lateral packing in the molecular level due to the strong stacking force. At high concentration (2 mg/mL), thin film was formed, while at moderate concentration (0.5 mg/mL) the polymer **P1** forms nanofibers with a diameter around 20 nm (Figure 8A). All fiber exhibited helical structure with a left-handedness (inset). At lower concentration of 0.2 mg/mL, the fiber tended to interweave together forming ring shape structures, i.e., coexisting of both nanofiber and nanorings (Figure 8B). While at a very dilute concentration (0.05 mg/mL), helical and well-dispersed nanorings with different morphologies were observed (Figure 8C). It is also supported by the bimodal distribution of aggregate sizes observed in DLS studies. Drop-casting from THF, $CHCl_3$, and toluene gave similar results, which indicated that the driving force came from the inherent properties of the polymer chain and not due to the environmental effect.

It is conceivable that steric hindrance among the adjacent substitutents along the polymer backbone induced helicity. Such helical fibers have been reported with oligothiophenes[93–96] and oligo(*p*-phenylenevinylene)s[97–100] with chiral center and/or hydrogen bonding. In our case, no chiral center or hydrogen-bonding functional groups were incorporated on the polymer backbone. First of all, the polymer backbone is nonlinear because of 2,5 linkages of thiophene groups on **P1** backbone. Second, the side chains are conjugated, long, and rigid in nature. The combined effect of both factors mentioned able leads to sterric crowding of side chains along the polymer backbone (see below), which then lead to a helical twist on the polymer backbone, as shown in the Figure 8D. So the rigid side-chain probably unifies the molecular structure of the polymer, making it bend only in one direction. Third, the strong stacking force further enhanced the formation of helical structures; obviously the more ordered packing originated from strong intermolecular interaction.

Because of the rigid backbone structure of the conjugated polymer and the nonpolar nature of the side chains, it is very difficult to obtain highly ordered packing of the conjugated polymers. High-resolution transmission electron microscopy (HRTEM) results showed that thin film of **P3** contained nanocrystalline domains simply by drop-casting the polymer solution onto copper grid, as shown in Figure 9. The domain size varied up to tens of nanometers. Electron diffraction study further confirmed its crystalline structure (Figure 9, inset). Initially, it is believed that this could be due to the presence of residual palladium catalyst as an impurity, but the EDX result excluded this possibility (Figure S6 in Supporting Information). In addition, repeated purification of the polymers did not change the polymer characteristics. Since the side chain of the polymer is nonpolar and the backbone is highly rigid, intermolecular $\pi-\pi$ stacking could be the only driving force. The *d*-spacing values calculated from diffraction pattern is about 2.6−3.1 nm, which was a bit deviated from the proposed interplanar spacing value obtained in powder XRD (3.7−4.2 nm). This may be due to the different sample preparations, as the packing of the polymer chains could be complicated and might not be unique. Further detailed morphology studies of the polymer and its nanocomposites are being explored in our laboratory and will be reported in a separate contribution.

Conclusion

A series of cross conjugated polymers were synthesized and fully characterized. All polymers were readily soluble in common organic solvents and thermally stable up to 250 °C. Powder XRD patterns showed an ordered packing structure for **P2** and **P3**. Especially, **P3** showed two peaks probably due to the different length of the alternative side chains. UV−vis

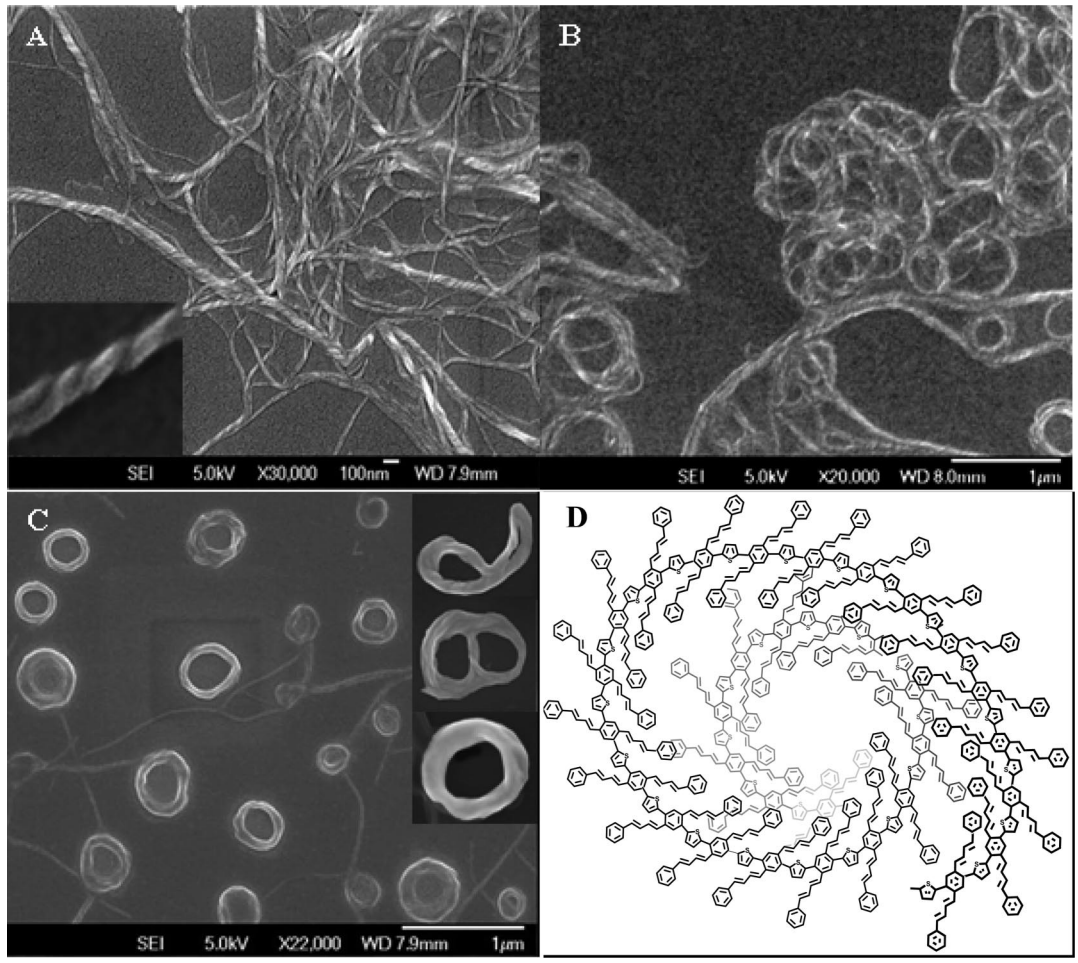

Figure 8. SEM images of **P1** drop-casted from toluene solutions of different concentrations onto glass plate: 0.5 mg/mL (A), 0.2 mg/mL (B), 0.05 mg/mL (C). Cartoon representing the helicity caused by the substituents along the polymer chain (D).

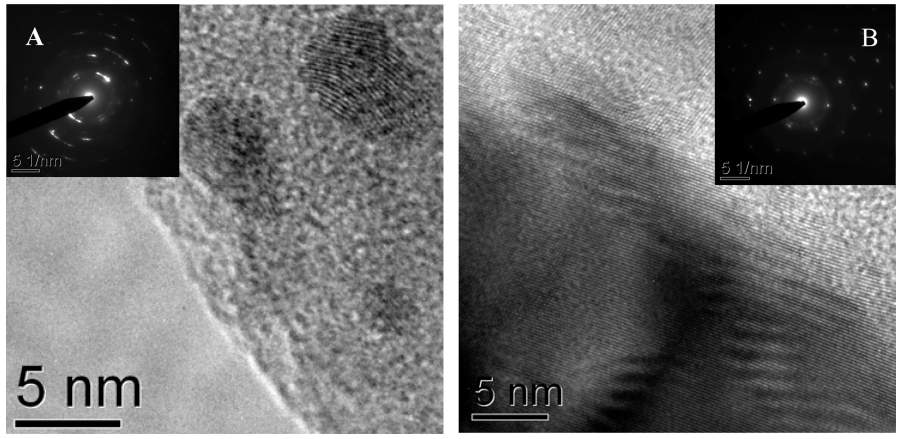

Figure 9. HRTEM images and electron diffraction patterns at crystalline domains of **P3** thin film.

spectra indicated the existence of absorption of intermolecular ground-state complex. Emission maxima showed a red shift with increasing concentration due to excimer formation. Quantum yields of polymers revealed the relationship between "soft" bisdiene side chain and rigid backbone. Large two-photon absorption (TPA) cross sections were observed due to extended conjugation and aligned "push−push" and "push−pull" structure. Intermolecular interaction was further confirmed by time-correlated single-photon counting (TCSPC). Solid phase studies showed that different self-assembly patterns were formed with different concentrations. Surprisingly, **P3** was able to form nanocrystalline phases via $\pi-\pi$ stacking force driven self-assembly.

Acknowledgment. The authors thank the Agency for Science and Technology Research and National University of Singapore for funding support. H. Li thanks the Nanoscience and Nanotechnology Initiative for a research scholarship. The technical support from the Department of Chemistry, National University of Singapore, is also acknowledged.

Supporting Information Available: Absorption, emission, excitation, DLS, and TCSPC spectra for all polymers. This

material is available free of charge via the Internet at http://pubs.acs.org.

References and Notes

(1) Sirringhaus, H.; Tessler, N.; Friend, R. H. *Science* **1998**, *280*, 1741.
(2) Friend, R. H.; Gymer, R. W.; Holmes, A. B.; Burroughes, J. H.; Marks, T. N.; Taliani, C. *Nature (London)* **1999**, *397*, 121.
(3) Garnier, F.; Hajlaoui, R.; Yassar, A.; Srivastava, P. *Science* **1994**, *265*, 1684.
(4) Antoniadis, H.; Hsieh, B. R.; Abkowitz, M. A.; Jenekhe, S. A.; Stolka, M. *Synth. Met.* **1994**, *62*, 265.
(5) Yu, G.; Heeger, A. J. *J. Appl. Phys.* **1995**, *78*, 4510.
(6) Li, H.; Valiyaveettil, S. *Macromolecules* **2007**, *40*, 6057.
(7) Hopf, H. *Angew. Chem., Int. Ed. Engl.* **1984**, *23*, 948.
(8) Hopf, H.; Maas, G. *Angew. Chem., Int. Ed. Engl.* **1992**, *31*, 931.
(9) Iyoda, M.; Hasegawa, M.; Miyake, Y. *Chem. Rev.* **2004**, *104*, 5085.
(10) Gorgues, A.; Hudhomme, P.; Salle, M. *Chem. Rev.* **2004**, *104*, 5151.
(11) Nielsen, M. B.; Diederich, F. *Chem. Rev.* **2005**, *105*, 1837.
(12) Buchan, C. M.; Cadogan, J. I. G.; Gosney, I.; henry, W. J. *J. Chem. Soc., Chem. Commun.* **1985**, 1785.
(13) Fielder, S.; Rowan, D. D.; Sherburn, M. S. *Angew. Chem., Int. Ed.* **2000**, *39*, 4331.
(14) van Walree, C, A.; Kaats-Richters, V. E. M.; Veen, S. J.; Wieczorek, B.; van der Wiel, J. H.; van der Wiel, B. C. *Eur. J. Org. Biomol. Chem* **2004**, *2*, 3432.
(15) Misaki, Y.; Matsumura, Y.; Sugimoto, T.; Yoshida, Z. *Tetrahedron Lett.* **1989**, *30*, 5289.
(16) Moore, A. J.; Bryce, M. R.; Skabara, P. J.; Batsanov, A. S.; Goldenberg, L. M.; Howard, J. A. K. *J. Chem. Soc., Perkin Trans. 1* **1997**, 3443.
(17) Zhao, Y.; Tykwinski, R. R. *J. Am. Chem. Soc.* **1999**, *121*, 458.
(18) Ciulei, S. C.; Tykwinski, R. R. *Org. Lett.* **2000**, *2*, 3607.
(19) Boldi, A. M.; Anthony, J.; Gramlich, V.; Knobler, C. B.; Boudon, C.; Gisselbrecht, J.-P.; Gross, M.; Diederich, F. *Helv. Chim. Acta* **1995**, *78*, 779.
(20) Zhao, Y.; McDonald, R.; Tykwinski, R. R. *J. Org. Chem.* **2002**, *67*, 2805.
(21) Moonen, N. N. P.; Pomerantz, W. C.; Gist, R.; Boudon, C.; Gisselbrecht, J.-P.; Kawai, T.; Kishioka, A.; Gross, M.; Irie, M.; Diederich, F. *Chem.—Eur. J.* **2005**, *11*, 3325.
(22) Klokkenburg, M.; Lutz, M.; Spek, A. L.; van der Maas, J. H.; van Walree, C. A. *Chem.—Eur. J.* **2003**, *9*, 3544.
(23) Mao, S. S. H.; Tilley, T. D. *J. Organomet. Chem.* **1996**, *521*, 425.
(24) Hörhold, H. H.; Helbig, M.; Raabe, D.; Opfermann, J.; Scherf, U.; Stockmann, R.; Weiss, D. Z. *Chem.* **1987**, *27*, 126.
(25) Eisler, S.; Tykwinski, R. R. *Angew. Chem., Int. Ed.* **1999**, *38*, 1940.
(26) Hopff, H.; Wick, A. K. *Helv. Chim. Acta* **1961**, *44*, 19.
(27) Köbrich, G.; Heinemann, H. *Angew. Chem., Int. Ed. Engl.* **1965**, *4*, 594.
(28) Iyoda, M.; Otani, H.; Oda, M.; Kai, Y.; Baba, Y.; Kasai, N. *J. Chem. Soc., Chem. Commun.* **1986**, 1794.
(29) Kozhushkov, S. I.; Leonov, A.; de Meijere, A. *Synthesis* **2003**, 956.
(30) Sakurai, H. *Pure Appl. Chem.* **1996**, *68*, 327.
(31) Matsuo, T.; Fure, H.; Sekiguchi, A. *Chem. Lett.* **1998**, 1101.
(32) Boldi, A. M.; Diederich, F. *Angew. Chem., Int. Ed. Engl.* **1994**, *33*, 468.
(33) Mitzel, F.; Boudon, C.; Gisselbrecht, J.-P.; Seiler, P.; Gross, M.; Diederich, F. *Chem. Commun.* **2003**, 1634.
(34) Hascoat, P.; Lorcy, D.; Robert, A.; Carlier, R.; Tallec, A.; Boubekeur, K.; Batail, P. *J. Org. Chem.* **1997**, *62*, 6086.
(35) Duan, Y.; Zhao, Y.; Chen, P.; Li, J.; Liu, S.; He, F.; Ma, Y. G. *Appl. Phys. Lett.* **2006**, *88*, 263503.
(36) Grunder, S.; Huber, R.; Horhoiu, V.; Gonzalez, M. T.; Schonenberger, C.; Calame, M.; Mayor, M. *J. Org. Chem.* **2007**, *72*, 8337.
(37) Oldham, W. J.; Lachicotte, R. J.; Bazan, G. C. *J. Am. Chem. Soc.* **1998**, *120*, 2987.
(38) Robinson, M. R.; Wang, S. J.; Heeger, A. J.; Bazan, G. C. *Adv. Funct. Mater.* **2001**, *11*, 413.
(39) Deb, S. K.; Maddux, T. M.; Yu, L. P. *J. Am. Chem. Soc.* **1997**, *119*, 9079.
(40) Maddux, T. M.; Li, W. J.; Yu, L. P. *J. Am. Chem. Soc.* **1997**, *119*, 844.
(41) Niazimbetova, Z. I.; Christian, H. Y.; Bhandari, Y. J.; Beyer, F. L.; Galvin, M. E. *J. Phys. Chem. B* **2004**, *108*, 8673.
(42) Fratilou, S.; Senthilkumar, K.; Grozema, F. C.; Christian-Pandya, H.; Niazimbetova, Z. I.; Bjandari, Y. J.; Galvin, M. E.; Siebbeles, L. D. A. *Chem. Mater.* **2006**, *18*, 2118.
(43) Wilson, J. N.; Josowicz, M.; Wang, Y. Q.; Bunz, U. H. F. *Chem. Commun.* **2004**, *24*, 2962.
(44) Preis, E.; Scherf, U. *Macromol. Rapid Commun.* **2006**, *27*, 1105.
(45) Zucchero, A. J.; Wilson, J. N.; Bunz, U. H. F. *J. Am. Chem. Soc.* **2006**, *128*, 11872.
(46) Zucchero, A. J.; Wilson, J. N.; South, C. R.; Bunz, U. H. F.; Weck, M. *Chem. Commun.* **2006**, *20*, 2141.
(47) Wilson, J. N.; Bunz, U. H. F. *J. Am. Chem. Soc.* **2005**, *127*, 4124.
(48) Otsubo, T.; Kohda, T.; Misumi, S. *Bull. Chem. Soc. Jpn.* **1980**, *53*, 512.
(49) Tietze, L. F. *Reactions and Synthesis in the Organic Chemistry Laboratory*; University Science: Mill Valley, CA, 1989; p 253.
(50) Baskar, C.; Lai, Y. H.; Valiyaveettil, S. *Macromolecules* **2001**, *34*, 6255.
(51) Wong, W. Y.; Choi, K. H.; Lu, G. L.; Shi, J. X.; Lai, P. Y.; Chan, S. M.; Lin, Z. Y. *Organometallics* **2001**, *20*, 5446.
(52) Smith, K.; James, D. M.; Mistry, A. G.; Bye, M. R.; Faulkner, D. J. *Tetrahedron* **1992**, *48*, 7479.
(53) Paliulis, O.; Ostrauskaite, J.; Gaidelis, V.; Jankauskas, V.; Strohriegl, P. *Macromol. Chem. Phys.* **2003**, *204*, 1706.
(54) Yasuda, T.; Yamamoto, T. *Macromolecules* **2003**, *36*, 7513.
(55) Yamamoto, T.; Saitoh, Y.; Anzai, K.; Fukumoto, H.; Yasuda, T.; Fujiwara, Y.; Choi, B. K.; Kubota, K.; Miyamae, T. *Macromolecules* **2003**, *36*, 6722.
(56) Jordan, E. F., Jr.; Feldeisen, D. W.; Wrigley, A. N. *J. Polym. Sci., Part A-1* **1971**, *9*, 1835.
(57) Hsieh, H. W.; Post, B.; Morawetz, H. *J. Polym. Sci., Polym. Phys. Ed.* **1976**, *14*, 1241.
(58) Liu, B.; Yu, W. L.; Lai, Y. H.; Huang, W. *Macromolecules* **2002**, *35*, 4975.
(59) Balanda, P. B.; Ramey, M. B.; Reynolds, J. R. *Macromolecules* **1999**, *32*, 3970.
(60) Lee, S. A.; Hotta, S.; Nakanish, F. *J. Phys. Chem. A* **2000**, *104*, 1827.
(61) Lamba, J. J. S.; Tour, J. M. *J. Am. Chem. Soc.* **1994**, *116*, 11723.
(62) Huang, W. Y.; Gao, W.; Kwei, T. K.; Okamoto, Y. *Macromolecules* **2001**, *34*, 1570.
(63) Shotwell, S.; Windscheif, P. M.; Smith, M. D.; Bunz, U. H. F. *Org. Lett.* **2004**, *6*, 4151.
(64) Skoog, D. A.; Holler, F. J.; Nieman, T. A. *Principle of Instrumental Analysis*, 5th ed.; Brooks/Cole: Pacific Grove, CA, 1998; p 359.
(65) Peng, K. Y.; Chen, S. A.; Fann, W. S. *J. Am. Chem. Soc.* **2001**, *123*, 11388.
(66) Sariciftci, N. S.; Smilowitz, L.; Heeger, A. J.; Wudl, F. *Science* **1992**, *258*, 1474.
(67) Theander, M.; Yartsev, A.; Zigmantas, D.; Sundstrom, V.; Mammo, W.; ersson, M. R.; Inganas, O. *Phys. Rev. B* **2000**, *61*, 12957.
(68) Jenekhe, S. A.; Osaheni, J. *Science* **1994**, *265*, 765.
(69) Halls, J. J. M.; Cornil, J.; dos Santos, D. A.; Silbey, R.; Hwang, D. H.; Holems, A. B.; Bredas, J. L.; Friend, R. H. *Phys. Rev. B* **1999**, *60*, 5721.
(70) Onoda, M.; Tada, K.; Zakhidov, A. A.; Yoshino, L. *Thin Solid Films* **1998**, *331*, 76.
(71) Yan, M.; Rothberg, L. J.; Kwock, E. K.; Miller, T. M. *Phys. Rev. Lett.* **1995**, *75*, 1992.
(72) Samuel, I. D. W.; Rumbles, G.; Collison, C. J. *Phys. Rev. B* **1995**, *52*, 11573.
(73) Dufresne, G.; Bouchard, J.; Belletête, M.; Durocher, G.; Leclerc, M. *Macromolecules* **2000**, *33*, 8252.
(74) Bouchard, J.; Belletête, M.; Durocher, G.; Leclerc, M. *Macromolecules* **2003**, *36*, 4624.
(75) Nesterov, E. E.; Zhu, Z.; Swager, T. M. *J. Am. Chem. Soc.* **2005**, *127*, 10083.
(76) Padmanaban, G.; Ramakrishnan, S. *J. Am. Chem. Soc.* **2000**, *122*, 2244.
(77) Siling, S. A.; Ronova, I. A.; Madii, V. A.; Lozinskaja, E. I.; Borisevich, Ju. E.; Vinogradova, S. V.; Kizel, V. A.; Reznichenko, A. V.; Kokin, V. N. *Synthesis and Properties of Heterocyclic Compounds*; Nova Science Publishers: Huntington, NY, 2001; p 115.
(78) Wang, C.; Liu, L.; Ma, W.; Zhou, Z.; Wang, G. Y.; Xu, Z. Z. *Optik* **2005**, *116*, 75.
(79) Demas, J. N.; Crosby, G. A. *J. Phys. Chem.* **1971**, *75*, 991.
(80) Xu, C.; Webb, W. W. *J. Opt. Soc. Am. B* **1996**, *13*, 481.
(81) Albota, M.; Beljonne, D.; Brédas, J. L.; Ehrlich, J. E.; Fu, J.-Y.; Heikal, A. A.; Hess, S. E.; Kogej, T.; Levin, M. D.; Marder, S. R.; McCord-Maughon, D.; Perry, J. W.; Röckel, H.; Rumi, M.; Subramaniam, G.; Webb, W. W.; Wu, X. L.; Xu, C. *Science* **1998**, *281*, 1653.
(82) Cumpston, B H.; Ananthavel, S. P.; Barlow, S.; Dyer, D. L.; Ehrlich, J. E.; Erskine, L. L.; Heikal, A. A.; Kuebler, S. M.; Sandy Lee, I.-Y.; McCord-Maughon, D.; Qin, J.; Röckel, H.; Rumi, M.; Wu, X. L.; Marder, S. R.; Perry, J. W. *Nature (London)* **1999**, *398*, 51.
(83) Tanihara, J.; Ogawa, K.; Kobuke, Y. *J. Photochem. Photobiol. A: Chem.* **2006**, *178*, 140.
(84) Drobizhev, M.; Karotki, A.; Kruk, M.; Rebane, A. *Chem. Phys. Lett.* **2002**, *355*, 175.
(85) Taylor, P. N.; Wylie, A. P.; Huuskonen, J.; Anderson, H. L. *Angew. Chem., Int. Ed.* **1998**, *37*, 986.

(86) Meyer, F.; Marder, S. R.; Pierce, B. M.; Bredas, J. L. *J. Am. Chem. Soc.* **1994***116*, 10703.
(87) Luo, Y.; Norman, P.; Macak, P. °; Agren, H. *J. Phys. Chem. A* **2000**, *104*, 4718.
(88) Wang, C. K.; Zhao, K.; Su, Y.; Ren, Y.; Zhao, X.; Luo, Y. *J. Chem. Phys.* **2003**, *119*, 1208.
(89) Nalwa, H. S.; Miyata, S. *Nonlinear Optics of Organic Molecules and Polymers*; CRC Press: Boca Raton, FL, 1997.
(90) Parthenopoulos, D A.; Rentzepis, P. M. *Science* **1989**, *245*, 843.
(91) Bhawalkar, J. D.; Kumar, N. D.; Zhao, C. F.; Prasad, P. N. *J. Clin. Laser Med. Surg.* **1997**, *15*, 201.
(92) Peng, K. Y.; Chen, S. A.; Fann, W. S. *J. Am. Chem. Soc.* **2001**, *123*, 11388.
(93) Kilbinger, A. F. M.; Schenning, A. P. H. J.; Goldoni, F.; Feast, W. J.; Meijer, E. W. *J. Am. Chem. Soc.* **2000**, *122*, 1820.
(94) Schenning, A. P. H. J.; Kilbinger, A. F M.; Biscarini, F.; Cavalini, M.; Cooper, H. J.; Derrick, P. J.; Feast, W. J.; Lazzaroni, R.; Leclère, Ph.; McDonnell, L. A.; Meijer, E. W.; Meskers, S. *J. Am. Chem. Soc.* **2002**, *124*, 1269.
(95) Leclère, P. H.; Surin, M.; Jonkheijm, P.; Henze, O.; Schenning, A. P. H. J.; Biscarini, F.; Grimsdale, A. C.; Feast, W. J.; Meijer, E. W.; Müllen, K.; Bredas, J. L.; Lazzaroni, R. *Eur. Polym. J.* **2004**, *40*, 885.
(96) Faid, K.; Leclerc, M. *J. Am. Chem. Soc.* **1998**, *120*, 5274.
(97) El-ghayoury, A.; Schenning, A. P. H. J.; van Hal, P. A.; van Duren, J. K. J.; Janssen, R. A. J.; Meijer, E. W. *Angew. Chem., Int. Ed.* **2001**, *40*, 3660.
(98) Schenning, A. P. H. J.; Jonkheijm, P.; Peeters, E.; Meijer, E. W. *J. Am. Chem. Soc.* **2001**, *123*, 409.
(99) Ajayaghosh, A.; George, S. J. *J. Am. Chem. Soc.* **2001**, *123*, 5148.
(100) Ajayaghosh, A.; Praveen, V. K. *Acc. Chem. Res.* **2007**, *40*, 644.

MA801506C